Combination of several spectral indexes and K-Means clustering to map the effects of an extreme flooding with Sentinel-2 imagery

Alonso Madrigal Sánchez [1], Jorge Antonio Silva Centeno [2]

[1] Dept. of Civil Engineering, Geo and Environmental Sciences, KIT, 76131 Karlsruhe, Germany – uyjqz@student.kit.edu
[2] Dept. of Geomatics, Federal University of Parana, 19001 Curitiba, Brazil – centeno@ufpr.br

Keywords: Remote Sensing, Flooding Management, GIS, MNDWI-NDVI, K-Means clustering.

ABSTRACT

Extreme flooding events increasingly threaten urban settlements, making advanced remote sensing approaches essential for effective monitoring and assessment. This study presents a novel methodology that combines multiple spectral indices with K-Means clustering to map flood extent and intensity using Sentinel-2 imagery, focusing on the extreme flooding event that affected Porto Alegre, Brazil, in April-May 2024. The approach integrates the water index MNDWI with complementary indices, including NDVI, NDWI, NIR, and SWIR bands. K-Means clustering was employed in two different ways: the fixed threshold approach and the automatic (adaptive) threshold determination, creating binary water/non-water classifications across the study area. The method demonstrated its ability to monitor temporal flood dynamics, revealing maximum water coverage during the peak flooding period. Both methodologies demonstrate high recall performance; however, the automatic adaptive threshold approach exhibits superior recall rates, achieving 93-97% across temporal periods. Precision rates for both methods remain moderate, primarily attributed to spectral confusion from wet soil, shadows, and urban features. The precision-recall trade-off analysis reveals a more balanced relationship for the adaptive threshold methodology. The water frequency classification illustrates the evolution of flooding by identifying areas that experienced early inundation and remained flooded over time. In contrast, the identification of persistent water bodies emphasises the consistency of water presence, offering a clear distinction between permanent and semi-permanent water bodies. The adaptive threshold multi-index methodology demonstrated superiority over the fixed threshold approach in complex mixed land-cover environments, offering robust flood intensity mapping capabilities that are crucial for disaster management and risk assessment in vulnerable riverbank communities.

1. Introduction

The stability of human settlements along riverbanks is severely compromised by extreme rainfall events, resulting in significant flooding that affects the population. The frequency of occurrence and intensity of flood events are increasing, making them one of the most pressing and widespread environmental threats, particularly in densely populated and poorly planned urban areas (United Nations Department of Economic and Social Affairs, 2024). On 22 April 2024, the Civil Defence of Brazil's Rio Grande do Sul state issued a meteorological alert indicating the risk of intense rainfall. This climatic event surpassed all previous historical extremes and impacted millions of people, with effects lasting several weeks (Simoes-Sousa et al., 2025). Water levels reached record highs, disrupting communication and affecting various infrastructures, including highways and the international airport in the capital city of Porto Alegre (Reis et al., 2021; Junior and Angelis, 2025).

The application of satellite imagery for studying and monitoring spatial-temporal changes in water resources plays a crucial and effective role in modern flood risk management, providing capabilities that traditional methods often lack (Li and Demir, 2024). Spectral indexes are useful to enhance information in a multispectral image. An index results from the arithmetic combination of several bands and enables the detection and mapping of specific targets on the Earth's surface. The most well-known index is the Normalised Difference Vegetation Index (NDVI), proposed by Townshend and Justice (1986) to help monitor and map vegetation, but indexes aimed at studying other targets, like water bodies, were also proposed.

The spatial-temporal changes in water resources can be primarily analysed through a water index derived from the image data. The Modified Normalised Difference Water Index (MNDWI), proposed by Xu (2006), offers enhanced visibility of open water features while significantly reducing interference from built-up areas, vegetation, and soil (Xu, 2006; Yılmaz, 2023). A combined water index method, such as NDVI MNDWI, is straightforwardly implemented and computationally efficient, suggesting its applicability for large-scale water detection challenges (Chen et al., 2020; Wu et al., 2021). Selecting an appropriate water index threshold is crucial for accurately distinguishing water from non-water features, directly influencing the accuracy and reliability of the results (Wu et al., 2021; Chen et al., 2015). The use of a multi-index approach highlights the potential strengths of each index while minimising their weak provides benefits over using a single index, particularly in hybrid regions and environments that include estuarine systems (Hwang and Um, 2015; Zhou et al., 2015).

The present study evaluates the reliability and effectiveness of a combined water index method for detecting water in flood areas. It focuses on integrating the Modified Normalised Difference Water Index (MNDWI) with the Normalised Difference Vegetation Index (NDVI) to better distinguish water bodies from other land cover types, especially in complex urban and estuarine settings. To achieve robust and reproducible results, two different approaches will be employed to establish an optimal index threshold for water classification. Initially, a fixed threshold is applied to the MNDWI, NDVI and other pertinent indexes constraints, such as vegetation index and different spectral bands. Subsequently, an adaptive threshold will be identified using K-Means clustering, which facilitates dynamic adjustments based on the spectral characteristics of the data. Additionally, the study investigates the influence of supplementary constraints, including terrain slope and size filtering, to further enhance the precision of water detection. The objective is to develop a methodology that effectively balances accuracy with computational efficiency, rendering it suitable for operational flood monitoring applications within resource-constrained settings.

2. Methodology

This study presents a comprehensive multi-step methodology for detecting, classifying, and analysing surface water dynamics using Sentinel-2 imagery. The approach combines multiple spectral indexes and constraints to optimise water detection accuracy, minimising individual index limitations through a computationally efficient, pixel-level processing framework suitable for large-scale analysis. The raster approach effectively manages high-resolution spatial datasets without requiring significant local computational resources

The research utilised Sentinel-2 Level-2A Surface Reflectance Harmonised data covering Porto Alegre, Brazil's metropolitan region, from April to September 2024, with less than 20% cloud cover. First, the images were downloaded, and water borders, urban areas, and the road networks were manually digitised within the QGIS software to obtain a ground truth validation set. Three spectral indices are computed and evaluated: the Normalised Difference Water Index (NDWI) proposed by McFeeters (1996), the Modified Normalised Difference Water Index (MNDWI) proposed by Xu (2006), and the Automated Water Extraction Index (AWEI), Feyisa et al. (2014), according to Equations 1-3.

$$NDWI = \frac{\text{Green}-\text{NIR}}{\text{Green}+\text{NIR}} \tag{1}$$

$$MNDWI = \frac{\text{Green}-\text{SWIR1}}{\text{Green}+\text{SWIR1}} \tag{2}$$

$$AWEI = 4(\text{Green} - \text{SWIR1}) - (0.25\ \text{NIR} + 2.75\ \text{SWIR1}) \tag{3}$$

The water-covered areas were delineated by applying these indexes, and the results were compared to the ground truth. The comparison revealed that the MNDWI produced better results, and it was selected as the primary water detection index due to its superior performance in complex mixed land cover environments. The worst results were obtained with AWEI due to its limitations in handling large areas and diverse land cover types.

Once it was determined that MNDWI was the most suitable water index, it was verified whether a unique threshold could be used to map water on different dates during the flood or if an adaptive threshold should be applied. It was verified whether an adaptive threshold can be automatically computed based on the available data. For this purpose, an automated K-Means clustering analysis was applied, assuming a bimodal MNDWI to create a binary map using 2 clusters (water and non-water pixels). The threshold values of these tests are presented in Table 1.

Subsequently, a fixed MNDWI threshold was applied based on established literature (see Table 2). As the results were not optimal, additional constraints in terms of NDWI and NDVI are introduced. The NDVI is the Normalised Difference Vegetation Index, proposed by Townshend and Justice (1986). The constraints are based on established literature recommendations presented in Table 2 (Chen et al., 2020; Lombana and Martínez-Graña, 2022). Additionally, the slope of the MNDWI is computed to avoid humid soil areas at the borders.

Table 1. MNDWI threshold value implemented for each period and for both approaches.

Period	Fixed	Adaptive
Apr-May	0.3	0.55
May-Jun	0.3	0.49
Jun-Jul	0.3	0.48
Jul-Aug	0.3	0.37
Aug-Sep	0.3	0.50

The approach incorporates fixed constraints, Table 2, including spectral band thresholds for Near Infrared (NIR) and Shortwave Infrared (SWIR), slope angle restrictions, vegetation masking using NDVI, and connected pixel analysis with minimum eight-pixel connectivity requirements (McCormack et al., 2022). This method recognises that effective water detection requires more than MNDWI values alone.

Table 2. Summary of conservative constraints applied for water detection.

Constraint & Index	Application	Threshold Value
Slope	Detection of Flat Areas	< 3°
SWIR1	Spectral Band B11	800
NIR	Spectral Band B8	1200
NDVI	Vegetation Index	0.05
NDWI	Water Index	0.4

Morphological operations, including dilation and erosion, are employed to remove noise and isolated pixels while preserving contiguous water bodies exceeding minimum size thresholds. For this purpose, a circular kernel of radius equal to 2 pixels is applied, and then the connected components transform is applied, considering 8 neighbours to identify small segments that were removed.

The analysis generates binary water masks for each temporal period, which are then combined to create water frequency maps that illustrate detection persistence across the five-month study period. These frequency maps categorise pixels into categories ranging from rare to permanent water occurrence based on their detection frequency. Additionally, binary masks are generated to identify water bodies that are consistently detected in at least three periods or all five periods. This multi-temporal approach effectively distinguishes between persistent water bodies and temporary flood-related features, offering a comprehensive representation of surface water dynamics suitable for monitoring large areas with complex land cover characteristics.

3. Results and Discussion

Figure 1 presents the MNDWI values obtained from four Sentinel-2 images taken during the flood event. Higher values, approaching +1, are indicative of water (represented in blue), while lower values, closer to -1, are more likely to be land or other surfaces (represented in red). The increment of water coverage is clearly observable in the plots, with the peak flooding period occurring in May-June, showing the maximum extent of water. MNDWI values that remain consistently negative suggest that the area is predominantly composed of non-water surfaces, whereas consistently positive MNDWI values indicate the presence of permanent water bodies.

The statistical analysis of the MNDWI (Table 3) shows negative mean values ranging from -0.40 to -0.51, confirming that non-water surfaces dominate the study area. Positive values occurred only in the upper percentiles (p90, p95, maximum), indicating that water bodies covered approximately 10-15% of the area. April-May exhibited moderate water presence with low variability ($\sigma = 0.27$), reflecting stable baseline conditions. In contrast, May-June, which coincides with peak flooding, recorded the highest variability ($\sigma = 0.44$), indicating increased spectral heterogeneity and making water-land separation more challenging. This complexity limited the applicability of a fixed threshold and favoured adaptive methods such as K-means clustering. Variability then decreased during August-September ($\sigma = 0.37 - 0.29$), consistent with floodwater recession.

Table 3. MNDWI Evaluation Metrics Summary by Time Period | Adaptive Approach

Period	***Mean***	***Std Dev***	***Min***	***Max***	***P90***	***P95***
Apr-May	-0.52	0.270	-0.96	0.99	-0.40	-0.26
May-Jun	-0.40	0.441	-1.0	1.0	0.37	0.89
Jun-Jul	-0.45	0.374	-1.0	1.0	-0.21	0.76
Jul-Aug	-0.45	0.298	-1.0	1.0	-0.19	0.16
Aug-Sep	-0.46	0.303	-0.90	0.99	-0.29	0.05

An example of the histogram of the MNDWI values is displayed in Figure 2, which exhibits a bimodal distribution: one peak for non-water surfaces between -0.6 and -0.7, and another peak for water surfaces between 0.8 and 1.0. Notably, the May–June histogram shows the widest positive peak (80,000-90,000 pixels, $\sigma = 0.44$), indicating spectral confusion with saturated surfaces, and accounting for the low precision (10%) and F1-score (0.18) in Table 4. The non-water peaks of Figure 2, remained stable but varied in width, with narrow peaks observed in April-May and August-September (~300,000–350,000 pixels), a broader peak (~450,000 pixels) in May-June, and the highest, sharpest peak (~500,000 pixels) in June-July, suggesting post-flood spectral stability. Due to space constraints, Figure 2 includes only one histogram, and the most pertinent details from the omitted histograms are summarised here.

The bimodal distribution effectively supports K-means clustering into two distinct groups (water and non-water) when applied to MNDWI values normalised to a range of 0–255. This approach has demonstrated greater adaptability and accuracy for the complex landscapes of Brazil compared to Otsu's fixed bimodal thresholding (Reis et al., 2021). A fixed MNDWI threshold of 0.30 proved to be overly conservative, leading to a significant number of false negatives and an underestimation of water extent, especially in the case of smaller water bodies. This observation is consistent with the findings of Acharya et al. (2018), who indicated that optimal threshold selection can improve accuracy and kappa coefficients. Additionally, it aligns with Reis et al. (2021), who proposed that adaptive thresholds help to reduce systematic classification errors.

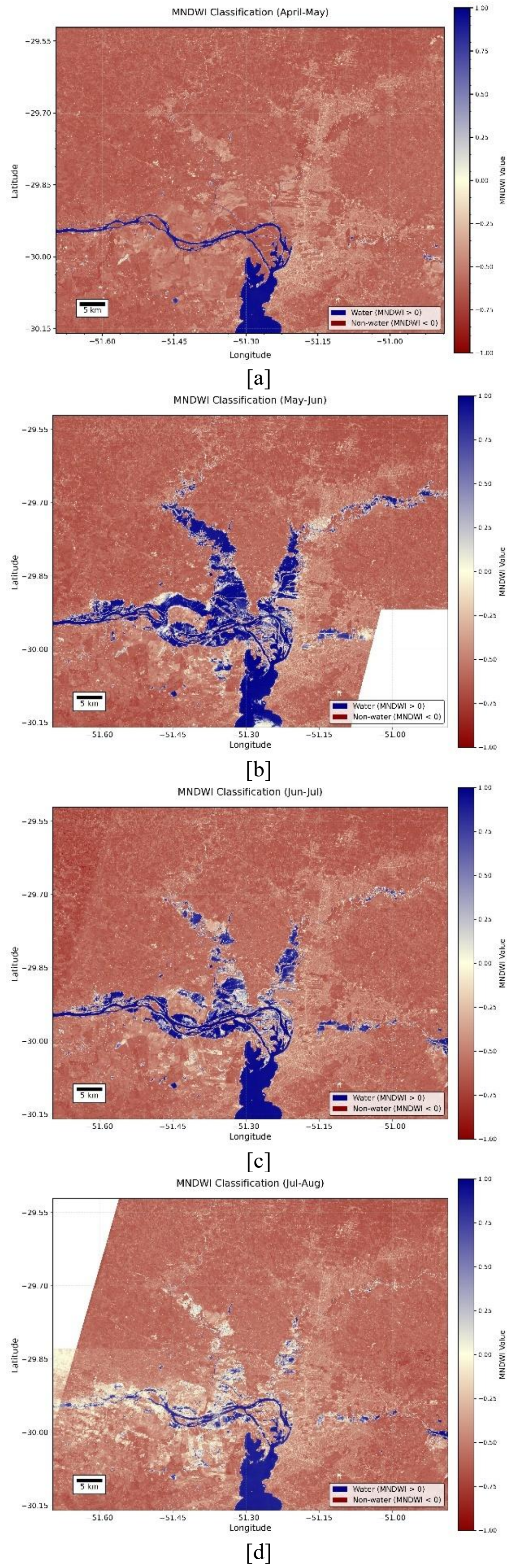

Figure 1. Plot of the raw MNDWI values for every pixel, with a range from -1 to 1, showing the peak of the flooding (Porto Alegre City, May-June 2024). (a) April-May; (b) May-June; (c) June-July; (d) July-August.

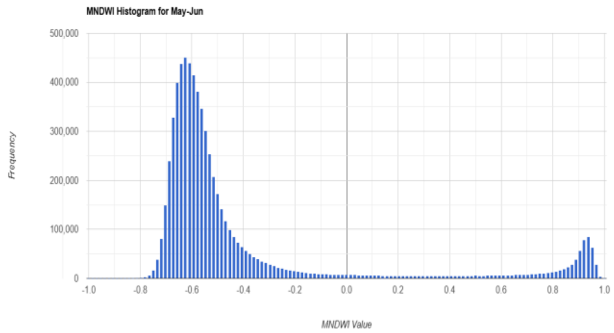

Figure 2. Histogram of the MNDWI values for the May-June period.

The incorporation of multiple spectral indices, including MNDWI, NDWI, and NDVI, enhanced the efficacy of water extraction within Porto Alegre's hybrid urban–agricultural landscape. These results are consistent with those reported by Yılmaz (2023) and show partial agreement with the findings of Zhou et al. (2015). Persistent spectral confusion was identified, including the misclassification of wet soil or mud as water, along with susceptibility to cloud and terrain shadows, and difficulties in distinguishing these areas from dark vegetation and built-up regions. These issues, also noted by Wu et al. (2021) and Chen et al. (2020), contributed to false negatives when combined with a conservative water mask.

Substantial temporal variability in water extent was evident throughout each study period and between the Fixed Approach (FA) and Adaptive Approach (AA), as illustrated in Figure 1. The April-May period was established as the baseline, with water extents of 148.9 km² (FA) and 161.5 km² (AA) detected. Maximum inundation occurred in May-June, reaching 428.2 km² (FA) and 456.8 km² (AA). Subsequently, water extent declined to 319.9 km² (FA) and 339.2 km² (AA) in June–July, 179.2 km² (FA) and 203.7 km² (AA) in July–August, before stabilising at 170.6 km² (FA) and 205.2 km² (AA) in August-September. Notably, the adaptive method consistently identified greater water extent, particularly under extreme flooding conditions.

Water detection metrics presented in Table 4 reveal a variable trade-off between precision and recall. The adaptive method produced higher recall values (up to 0.97) and robust F1-scores, particularly during extreme flood conditions in May–June. However, this improvement came with some trade-offs: adaptive thresholding sometimes resulted in slightly lower precision (0.10–0.31) and higher RMSE values, indicating a rise in false positive classifications and slightly less precise spatial delineation. Despite this, the adaptive method generally produced higher F1-scores and maintained reliable detection across temporal variations. In contrast, the fixed approach achieved marginally higher precision and fewer false positives, thereby enhancing overall accuracy under stable hydrological conditions. The high overall classification accuracy can be misleading due to class imbalance, as only about 4.5% of the total study area is classified as water. As noted by Chen et al. (2015), such imbalances can lead to inflated accuracy scores that do not reflect true detection performance. This trade-off is acceptable for flood monitoring applications where missing actual flooding (false negatives) is more critical than occasional over-detection (false positives). The Kappa coefficient (ranging from 0.18 to 0.45) is also sensitive to class imbalance, as water bodies constitute a small area. RMSE analysis supports these findings, showing the highest spatial accuracy in April–May (RMSE: 0.14–0.15) and the lowest in May–June (RMSE: 0.28–0.29), indicating greater boundary errors during peak flooding (see Table 5).

Table 4. Classification performance metrics comparisons: Precision, Recall, and F1-Score for Water Detection Model

Period	**Precision**		**Recall**		**F1-Score**	
	FA	***AA***	***FA***	***AA***	***FA***	***AA***
Apr-May	0.31	0.31	0.84	0.93	0.46	0.47
May-Jun	0.11	0.10	0.85	0.96	0.20	0.18
Jun-Jul	0.15	0.13	0.86	0.97	0.25	0.23
Jul-Aug	0.26	0.21	0.82	0.95	0.39	0.34
Aug-Sep	0.28	0.24	0.85	0.96	0.42	0.39

The number of true positives (TP), false positives (FP) and false negatives (FN) were computed for each period, as displayed in Table 6. The values reveal that the adaptive method improved true positive detection by ~10% and reduced false negatives by 50-80% compared to the fixed approach. However, this came at the cost of up to 111 km² more false positives during May–June, lowering precision. These findings align with Feyisa et al. (2014), which emphasised the spectral confusion that often arises between water and saturated surfaces, particularly within heterogeneous land cover environments

Table 5. Model performance metrics comparisons: Overall Accuracy (OA), Kappa Coefficient (KC), and RMSE for water detection model.

Period	**OA**		**KC**		**RMSE**	
	FA	***AA***	***FA***	***AA***	***FA***	***AA***
Apr-May	0.98	0.98	0.45	0.46	0.14	0.15
May-Jun	0.93	0.91	0.18	0.17	0.28	0.29
Jun-Jul	0.95	0.94	0.24	0.22	0.24	0.25
Jul-Aug	0.97	0.96	0.38	0.33	0.18	0.19
Aug-Sep	0.98	0.97	0.41	0.38	0.16	0.18

True negative (TN) information was intentionally excluded from Table 6, as it is deemed less relevant in this context. The class imbalance makes non-water classification significantly easier and more abundant, rendering TN ineffective in distinguishing between good and poor water detection performance. Consequently, metrics such as precision, recall, and F1-score (which emphasise the minority class, water) are much more informative for this study.

Each MNDWI water mask was subsequently binarised and aggregated to visualise flood dynamics. Water frequency classification, Figure 3, employs a multi-class methodology to systematically categorise areas based on the frequency of water detection (0-5 detections) throughout the study period, thus revealing the temporal evolution of the flood and spatial patterns of flood persistence. Permanent water (5/5 detections) corresponds to major rivers and lagoons, while frequent (3-4 detections) and seasonal (3 detections) water align with floodplains and locations with compromised drainage capacity. Occasional (1-2 detections) and rare (1 detection) waters reflect transient flooding or possible false positives, requiring careful interpretation. Spectral detection issues and mixed pixel effects can lead to inconsistent identification of water, as the MNDWI index may struggle to differentiate between water, wet soil, mud, and shadows, resulting in potential misclassifications (Feyisa et al., 2014; Wu et al., 2021).

Table 6. MNDWI performance metrics for each period: comparison between the Fixed (FA) & Adaptive (AA) approaches

Period	TP (Km²)		TN (Km²)		FN (Km²)	
	FA	*AA*	*FA*	*AA*	*FA*	*AA*
Apr-May	54.2	60.06	118.4	131	10.3	4.50
May-Jun	54.8	62.25	441	552.2	9.74	2.31
Jun-Jul	55.3	62.59	315.2	406.8	9.25	1.97
Jul-Aug	53.1	61.41	154.6	238	11.5	3.14
Aug-Sep	55	61.89	142.8	194.1	9.61	2.67

The identification of persistent water bodies, illustrated in Figure 4, employs a binary classification framework to delineate specific areas. The output is a clear water/non-water mask that highlights stable water features consistently present over defined temporal criteria. For instance, Figure 4a specifically, it shows pixels classified as water during all observation periods, ensuring that only unequivocally permanent water bodies, such as the main river, are designated as permanent water. This methodology classifies pixels based on the detection of persistent water bodies across all temporal periods. One of its significant applications is identifying key hydrological features and validating the spatial patterns observed in frequency classification (Xu, 2006). Nevertheless, this method also reveals limitations in detecting occasional and rare classes (Figure 4b and c, respectively), which may result from temporary ponding, mixed pixels, or spectral misclassification (Feyisa et al., 2014; Wu et al., 2021). The precision-recall trade-off inherent in threshold-based classification approaches requires careful consideration when interpreting results, particularly in zones with ambiguous spectral signatures (Acharya et al., 2018; Reis et al., 2021).

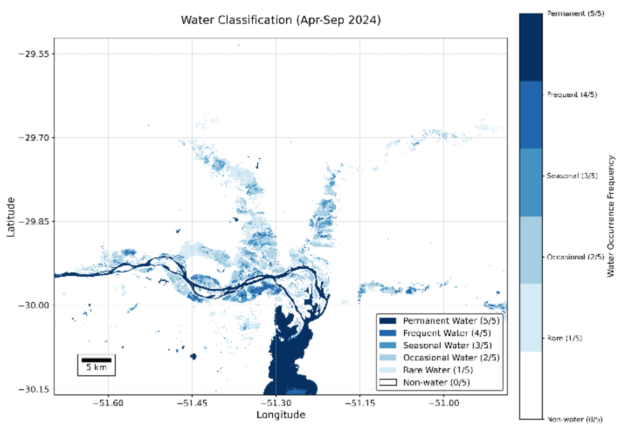

Figure 3. Water Frequency Classification. It shows the weighted frequency map of water detection, with areas classified based on the detection frequency (0-5). This classification encompasses data collected over the entire period, April to September 2024.

4. Conclusion

In the present study, the temporal dynamics of a severe flood event were systematically mapped. To achieve this objective, a comparative analysis was conducted employing two distinct methodological approaches: one utilising an adaptive threshold applied to the MNDWI, and the other employing a fixed threshold, also based on MNDWI. Both methodologies integrated multiple spectral bands and indices to delineate the flooded areas effectively. The application of the K-Means clustering proved to be feasible to compute an adaptive threshold; nevertheless, better results were obtained by combining several indexes and spectral bands. The method enhances water detection across the complete flood cycle, including initial inundation, peak extent, and recession phases.

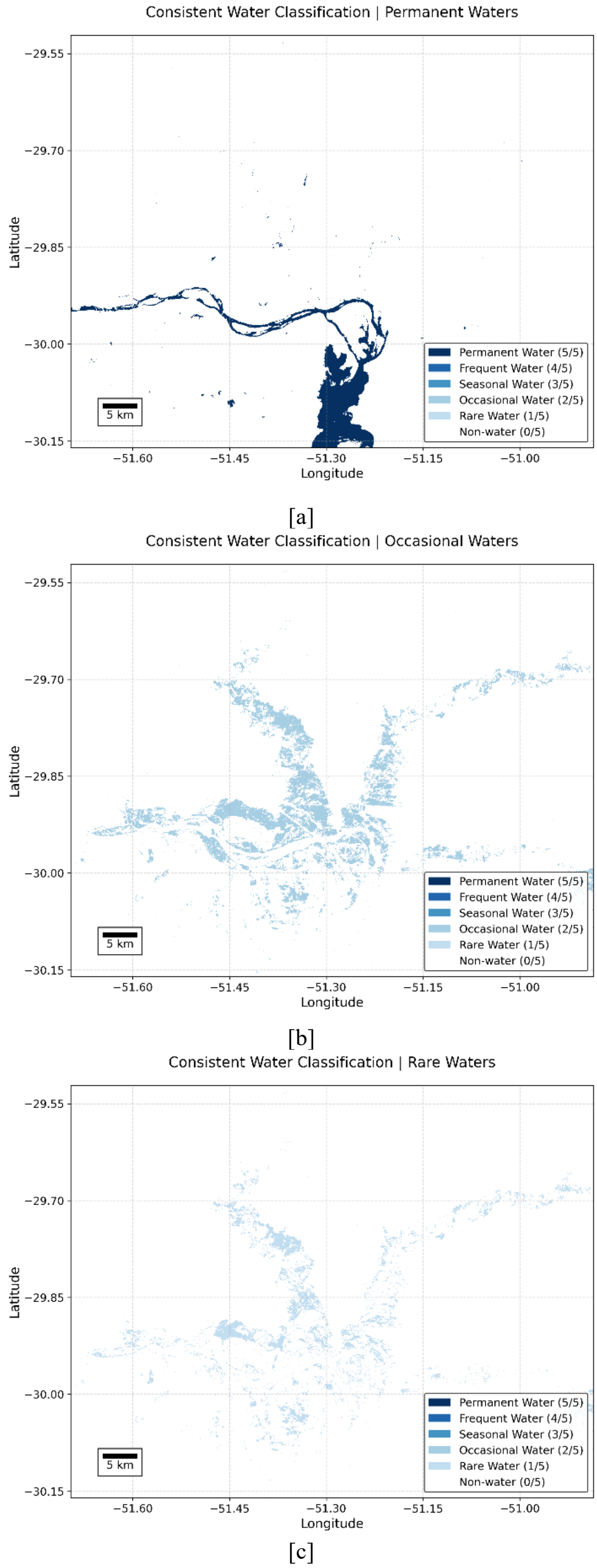

Figure 4. Plot of the consistent water classification approach showing the progression of the flooding: (a) Permanent Waters, (b) Occasional Water, (c) Rare Water.

Results reveal a distinct precision-recall trade-off between adaptive and fixed thresholding methods. The adaptive approach prioritises recall and reduces false negatives, crucial for flood monitoring, while the fixed method prioritises precision and reduces false positives. Variability in water levels during May June underscores the need for adaptable thresholding strategies due to spectral complexities. Although the methodology performs well in moderate conditions, extreme flooding can lead to spectral confusion, increasing false positives. This highlights the limitations of static thresholding and suggests the need for dynamic adjustment mechanisms to reduce both commission and omission errors.

The temporal compositing framework generates multi-class water frequency maps that indicate persistence levels, aiding flood risk assessment. However, caution is advised when interpreting rare water classes due to potential detection uncertainties. In summary, this study offers an efficient framework for operational flood monitoring in mixed urban agricultural environments, suggesting future research focus on refining adaptive thresholding, incorporating high-resolution imagery and hydrological data, and improving validation processes.

5. Acknowledgements

The authors would like to express their gratitude to Karlsruhe Institute of Technology [KIT], particularly the Institute of Photogrammetry and Remote Sensing and the Geodetic Institute, for providing the facilities and academic environment that facilitated this research. Special appreciation is extended to Dr.-Ing. Sylvia Marlene Hochstuhl for her invaluable guidance, constructive feedback, and continuous support throughout the completion of this paper.

6. References

Acharya, T. D., Subedi, A., Lee, D. H., 2018. Evaluation of Water Indices for Surface Water Extraction in a Landsat 8 Scene of Nepal. *Sensors*, 18.

Bian, F., Xie, Y. (eds), Geo-Informatics in Resource Management and Sustainable Ecosystem. *GRMSE 2014, Communications in Computer and Information Science*, 482, Springer, Berlin, Heidelberg, 482–491.

Chen, F., Chen, X., de Voorde, T., Roberts, D., Jiang, H., Xu, W., 2020. Open water detection in urban environments using high spatial resolution remote sensing imagery. *Remote Sensing of Environment*, 242, 111706.

Chen, Y., Zhou, H., Zhang, H., Du, G., Zhou, J., 2015. Urban flood risk warning under rapid urbanisation. *Environmental Research*, 139, 3-10.

Feyisa, G. L., Meilby, H., Fensholt, R., Proud, S. R., 2014. Automated Water Extraction Index: A new technique for surface water mapping using Landsat imagery. *Remote Sensing of Environment*, 140, 23-35.

Hwang, Y. S., Um, J.-S., 2015. Monitoring the Desiccation of Inland Wetland by Combining MNDWI and NDVI: A Case Study of Upo Wetland in South Korea. *Journal of Korea Spatial Information Society*, 23(6), 31-41.

Junior, M., Angelis, C., 2025. An Analysis of Hydrodynamic Models and the Agriculture-Climate Change Relationship in Rio Grande Do Sul Floods. *Hydrology*.

Li, Z., Demir, I., 2024. Flood sequence mapping with multimodal remote sensing under the influence of dense vegetation. *International Journal of Remote Sensing*, 45(4), 1059-1078.

Lombana, L., Martínez-Graña, A., 2022. A Flood Mapping Method for Land Use Management in Small-Size Water Bodies: Validation of Spectral Indexes and a Machine Learning Technique. *Agronomy*, 12(6), 1280.

McCormack, T., Campanya, J., Naughton, O., 2022. A methodology for mapping annual flood extent using multi-temporal Sentinel-1 imagery. *Remote Sensing of Environment*, 282.

McFeeters, S. K., 1996. The use of the Normalized Difference Water Index (NDWI) in the delineation of open water features. *International Journal of Remote Sensing*, 17(7), 1425-1432.

Reis, L. G. M., Souza, W. d. O., Ribeiro Neto, A., Fragoso, C. R., Ruiz-Armenteros, A. M., Cabral, J. J. d. S. P., Montenegro, S. M. G. L., 2021. Uncertainties Involved in the Use of Thresholds for the Detection of Water Bodies in Multitemporal Analysis from Landsat-8 and Sentinel-2 Images. *Sensors*.

Simoes-Sousa, I., Camargo, C. M. L., Ta´vora, J., Piffer-Braga, A., Farrar, J., Pavelsky, T., 2025. The May 2024 Flood Disaster in Southern Brazil: Causes, Impacts, and SWOT-Based Volume Estimation. *Geophysical Research Letters*, 52.

Townshend, J. R., Justice, C. O., 1986. Analysis of the dynamics of African vegetation using the normalized difference vegetation index. *International Journal of Remote Sensing*, 7(11), 1435-1445.

United Nations Department of Economic and Social Affairs, 2024. World population prospects: Data sources.

Wu, X., Wu, B., Wu, Y., Zhang, Q., 2021. Enhancement of Water Index Feature of Satellite Image in Mountainous Areas with Slope Information. *Journal of the Indian Society of Remote Sensing*, 49, 1109-1120.

Xu, H., 2006. Modification of normalised difference water index (NDWI) to enhance open water features in remotely sensed imagery. *International Journal of Remote Sensing*, 27(14), 3025-3033.

Yılmaz, O. S., 2023. Automatic detection of water surfaces using K-means++ clustering algorithm with Landsat-9 and Sentinel-2 images on the Google Earth Engine Platform. *Bilge International Journal of Science and Technology Research*, 7(2), 105-111.

Zhou, W., Li, Z., Ji, S., Hua, C., Fan, W., 2015. A new index model NDVI-MNDWI for water object extraction in hybrid area.